Methods of extracting ISGRI spectra

Piotr Lubiński (CAMK, Warsaw & ISDC), Masha Chernyakova (ISDC), Peter Kretschmar (MPI, Garching & ISDC), Nicolas Produit (ISDC), Jerome Rodriguez (CEA, Saclay & ISDC), Simona Soldi (ISDC), Roland Walter (ISDC)

1. Methods

Besides the standard method of extracting ISGRI spectra there are alternative possibilities to produce spectra, using the fluxes from sky images. These alternative methods are used occasionally, mainly for weaker sources, which cannot be detected in a single science window. In this case the standard method, if not forced, will not extract spectra. Since fluxes in images and those in standard spectra are calculated in a different way with background treated in a different manner, the results of both approaches may diverge. Such a divergence may lead to a false result after applying some of these methods, in particular for weaker objects, with low signal to noise ratio. This report presents results of the first tests of 5 different methods used to prepare ISGRI spectra for sources with brightness ranging from 1 Crab to about 10 mCrab.

There are two groups of methods which are studied below, one based on the standard spectral extraction within OSA level SPE, and the second, where the spectrum is prepared using flux results from images. For the standard spectral extraction there is a possibility to choose between ii_spectra_extract and ii_spectral executables, setting parameter 'method' to 1 or 2, respectively. The second choice may be done in two ways, depending on which PIF files are used, from standard ('method' = 1) or from alternative ('method' = 2) pipeline. In this report for ii_spectral based extraction we present only results obtained with its default PIF selection from the alternative pipeline.

A method making the use of fluxes extracted from individual science window images is recommended as the best one among all procedures based on image results (A. Gros, private comm.). Final spectrum is composed of mean fluxes for sky pixel at the catalog source position, calculated for Science Windows merged in given observation.

Methods based on mosaic images may be affected by the imperfections of the mosaic construction, especially when the sky images come from quite distant pointings, as it is in the case of GPS survey. On the other hand, mosaic image, with its large exposure, contains data with reduced statistical uncertainties. Alternatively, instead using the fluxes observed for a given sky pixel one may construct the spectrum with fluxes determined for a given source during mosaicing step, i.e., from isgri_mosa_res.fits file.

All tested methods are listed in Table 1, also the notation used later is defined there. Image and spectral extraction was done with OSA package, in version pre-4.2 (17.11.2004). For mosaicing step, parameter OBS1_PixSpread was set to zero. The spectra were extracted for 13 energy bins:

13-22.1, 22.1-25.9, 25.9-30.2, 30.2-40.3, 40.3-51.3, 51.3-63.3, 63.3-70.9, 70.9-80.0, 80.0-104.9, 104.9-149.9, 149.9-250.0, 250.0-520.9 and 520.9-993.4 keV. These bins were selected to match the regions with or without lines observed in ISGRI background spectrum.

Table 1: Tested methods.

Method	Data used	Executable
S1	PIF, scws spectra, 'method' = 1	ii_spectra_extract
IA	average of fluxes from sky images	ii_skyimage
MI	fluxes from mosaic image	ii_skyimage
MR	fluxes from mosaic results	ii_skyimage
S2	PIF, scws spectra, 'method' = 2	ii_spectral

2. Crab

In the beginning, all methods were applied to Crab observations. For this strong, steady source with well established spectral model, differences between tested spectra should be reduced to systematic effects. Also influence of offset angle on results was tested for that source. List of all Crab data sets is presented in Table 2.

An example of test results obtained for Crab observed in Revs. 0044, 0102 and 0239 is shown in Figure 1, where the relative fluxes extracted with alternative methods are compared. Method S1 fluxes were used as a reference normalization. Compared to the standard spectral extraction method all other methods produce usually smaller fluxes, with except for staring observation with ≈ 0 degrees offset. The observed flux reduction is almost always smallest for method based on mosaic results, MR. Fluxes prepared with image flux averaging, IA, appear to be very close to MR results sometimes matching them and sometimes lying below. Method using mosaic image, MI, gives lower values, this difference sometimes reaches ≈ 15 %. At last, alternative spectral extraction S2 always shows the lowest fluxes, what at most comes from the lower PIF values than those computed within S1 pipeline. Also lack of the correction for absorption in NOMEX layer supporting IBIS mask is seen for S2 at lower energy bands.

In the range 22-250 keV methods S1, IA and MR are in agreement within 10 % range for all Crab data with < 10 degrees offset angle. Differences observed for fluxes obtained with different methods do not correlate with the offset angle. Moreover, all methods seem to give the same spectral slope. For higher energies fluxes determined with method S1 are almost always larger and this excess increases with increasing offset angle.

Spectra obtained for Crab with methods S1, IA, MI and MR were compared in a more quantitative way via fitting to them a power law model. In fitting 22-250 keV energy range was used and

Table 2: Crab data sets used for tests. Mean offset angle was calculated as a mean weighted with the exposure time.

Source	Rev.	Exposure ks	Offset range deg	Mean offset deg	Flux in 30-40 keV counts/s
Crab	0039	73.4	0	0	38.9
Crab	0043	65.7	0-2.9	1.9	38.2
Crab	0043	109.7	0-5.7	3.0	38.0
Crab	0043	28.3	10.4	10.4	39.7
Crab	0044	38.0	0-2.8	2.1	38.3
Crab	0044	123.1	0-6.0	3.7	37.7
Crab	0044	131.0	0-6.6	3.8	37.7
Crab	0044	90.6	3.1-6.6	4.6	37.9
Crab	0102	20.1	0.15	0.15	37.6
Crab	0102	68.0	0.15-5.8	2.2	37.7
Crab	0102	42.6	13.6	13.6	40.7
Crab	0102	43.6	14.6	14.6	35.1
Crab	0170	19.3	0.15-3.0	2.1	38.0
Crab	0170	48.0	0.15-5.9	3.5	37.8
Crab	0170	58.1	0.15-9.9	4.2	37.9
Crab	0170	28.6	4.2-9.9	5.9	38.1
Crab	0170	24.4	13.8-28.2	17.8	31.5
Crab	0239	42.7	0.15-2.8	1.4	37.7
Crab	0239	130.1	0.15-5.9	3.2	37.6
Crab	0239	85.9	3.0-5.9	4.1	37.5
Crab	0239	66.0	3.8-4.5	4.0	37.5

only statistical errors were apllied. Response matrix was prepared by rebinning the latest RMF matrix isgr_rmf_grp_0012.fits, also the latest ARF file, isgr_arf_rsp_0006.fist was used. The results of these tests are summarized in Tables 3 and 4, where fitted power law index and 20-100 keV model fluxes are presented. In the last row of these Tables a mean value for each method is shown. All methods give almost exactly the same spectral index, although this quantity varies within 3 % range for different Crab observations. Standard method S1 produces the largest fluxes, mosaic results method MR is very close (3 %), shortly then comes method IA (image fluxes averaging), mosaic image method MI exhibits mean fluxes about 8 % lower than those obtained with method S1.

Differences between fluxes determined with various methods are under studies. At this moment

Table 3: Power law index fitted for Crab spectra extracted with different methods. Typical error: 0.002

Rev.	Offset	S1	IA	MI	MR
0039	0	2.223	2.219	2.219	2.224
0043	0-2.9	2.264	2.263	2.265	2.264
0043	0-5.7	2.266	2.264	2.265	2.264
0044	0-2.8	2.275	2.271	2.274	2.270
0044	0-6.0	2.275	2.270	2.269	2.269
0044	0-6.6	2.276	2.271	2.272	2.270
0044	3.1-6.6	2.277	2.271	2.272	2.271
0102	0.15	2.223	2.224	2.224	2.228
0102	0.15-5.8	2.235	2.235	2.236	2.238
0170	0.15-3.0	2.236	2.234	2.231	2.234
0170	0.15-5.9	2.234	2.233	2.230	2.233
0170	0.15-9.9	2.222	2.229	2.229	2.229
0170	4.2-9.9	2.210	2.222	2.220	2.221
0239	0.15-2.8	2.261	2.258	2.261	2.260
0239	0.15-5.9	2.254	2.253	2.254	2.252
0239	3.0-5.9	2.250	2.249	2.250	2.248
Mean	—	2.249	2.248	2.248	2.248

the deviation between standard method S1 and weighted mean method IA seems to be understood. In the upper panel of Figure 2 count rates obtained for 30-40 keV band are presented for all Science Windows from Crab observation during Rev. 0239, with offset angle in 0.15-5.9 degrees. range. Variations observed for S1 results are much smaller than those for method IA. For comparison, also fluxes obtained via fitting PSF for each ScW image are shown there, and they are in agreement with the standard method data. The middle panel of Figure 2 presents the distribution of count rates measured with methods S1 and IA, results of the latter method are spread on a broader range. At last, in the lower panel of Figure 2 the ratio between IA and S1 count rates is plotted against the area ratio. Area ratio in this case is the ratio of areas of the sky pixel, having the source catalog position inside, and the hypothetical pixel centered exactly at the source position. This ratio should be correlated with the deviation between the flux fitted with PSF for the source not necessarily located at the sky pixel centre and the flux ascribed to that pixel in the image. As can be seen, there is a clear correlation between the IA/S1 flux ratios and area ratios.

Since the discrepancies observed in the upper panel of Figure 2 exceed sometimes 10 % it is necessary to correct the results of method IA for this effect. Before such a correction will

Table 4: Model flux in 20-100 keV range for Crab spectra extracted with different methods. Units: photons cm^{-2} s^{-1}, typical error: 0.002

Rev.	Offset	S1	IA	MI	MR
0039	0	0.267	0.266	0.243	0.266
0043	0-2.9	0.261	0.254	0.231	0.244
0043	0-5.7	0.260	0.253	0.246	0.251
0044	0-2.8	0.264	0.252	0.241	0.254
0044	0-6.0	0.260	0.249	0.239	0.248
0044	0-6.6	0.261	0.249	0.224	0.249
0044	3.1-6.6	0.262	0.250	0.230	0.253
0102	0.15	0.257	0.257	0.257	0.262
0102	0.15-5.8	0.259	0.251	0.245	0.256
0170	0.15-3.0	0.260	0.247	0.238	0.248
0170	0.15-5.9	0.258	0.247	0.230	0.252
0170	0.15-9.9	0.258	0.247	0.244	0.251
0170	4.2-9.9	0.256	0.244	0.228	0.248
0239	0.15-2.8	0.258	0.248	0.238	0.251
0239	0.15-5.9	0.256	0.245	0.233	0.245
0239	3.0-5.9	0.255	0.243	0.233	0.246
Mean	—	0.259	0.250	0.237	0.251

be applied in OSA analysis software, one may correct IA count rates using the curve fitted to observed distribution of IA/S1 ratios along pixel area ratios axis. Figure 3 shows the results of this phenomenological correction done after fitting the second order polynomial to all IA/S1 ratios obtained for 8 energy bands data of Rev. 0239. Fitted parameters are: 1.34211, -0.72736 and 0.35878 for the zero-th, first and second polynomial component, respectively.

The discrepancies between mean fluxes obtained from ScW sky images (IA) and fluxes determined from mosaic sky image (MI) or from mosaic PSF fitting (MR) will be studied in future. Also the dependence of the S1 and IA fluxes on the offset angle for larger offset angles is under evaluation. The lowest panel of Figure 1 shows that the situation is more complicated when the source is located at ≥ 10 degrees from the sky image centre.

2.1. Moderate and weak sources

Spectral extraction for weaker sources was done only with methods S1, IA and MI. Among these object only one, Mrk 509, was observed in staring mode (Rev. 0070). The rest of sources was found in GPS data from Revs. 0100 and 0116, 0118. Basic information on the tested data is collected in Table 5. The strength of objects is compared in two last columns, in absolute and mCrab values.

The spectra extracted with different methods for weaker objects are compared in Figures 4-6. Results for Mrk 509 (Fig. 4) are not affected by the offset angle effects. In this case all methods are in good agreement, although the source is very weak. On the other hand, GPS data are always obtained for pointings spanning large range of offset angles for a given source. This affects the results even for quite strong objects, as it is shown in Figure 5, where S1 fluxes are larger than those from images extracted for data from Rev. 0100 and smaller for data from Revs. 0116,0118. This case illustrates the same type of behaviour which was already shown for 10.4 degrees offset Crab observation from Rev. 0043. Depending on the distribution of the source position in individual ScW sky images one may obtain various results for the mean or mosaic spectrum. The natural explanation of these discrepancies is the non-uniform efficiency of the detector plane and non-uniform background distribution over the detector area. Therefore, future studies of these effects will be done together with the non-uniformity investigations.

The last Figure, 6, presents yet another effect, this time influencing seemingly only the standard method spectra. When the object is observed at large offset angles, the count rates derived with method S1 for smaller signal-to-noise-ratio data are obviously too large, producing quite hard spectra. For comparison, background spectra obtained for the same ScWs set are shown in this Figure. This shows that the standard method, based on PIFs, is much more sensitive to the background non-uniformity on the edges of detector area. Presumably this is the result of applying this method when the object was not detected and the background fluctuations are mixed with the source fluxes.

Table 5: Data for weaker objects used for tests. Average count rate for Crab in 30-40 keV, equal to 38 counts/s, was used to calculate the relative fluxes.

Source	Rev.	Exposure ks	Offset deg	Mean offset deg	Flux in counts/s	30-40 keV mCrab
Mrk 509	0070	52.6	0	0	0.27	7
4U 1700-377	0100	96.7	1.1-12.4	7.3	5.0	132
4U 1700-377	0116,0118	26.5	6.1-15.1	10.6	10.6	279
H 1538-522	0100	49.1	11.4-21.6	17.3	1.1	29
H 1538-522	0116,0118	72.0	5.2-23.1	14.6	1.1	29

3. Conclusions

Systematic differences between various ISGRI spectral exctraction methods were studied on the Crab data. The standard spectral extraction produces the largest fluxes. Average fluxes computed with method based on mean flux from sky images and method using mosaic results are lower than those from the standard method by about 3%. For method extracting directly fluxes from mosaic images this discrepancy is larger, about 8%. The lowest fluxes are produced with spectral method 2, also the spectral shape is distorted in this case due to the lack of NOMEX absorption correction. There is no correlation between the offset angle and the observed deviation of alternative methods fluxes from 'standard' fluxes, for offset angles not exceeding ≈ 10 degrees and for energies below 250 keV. All methods based on image results lead to a similar relative spectral shape when compared with the standard method.

When the source is observed at larger offset angles, results of all methods seem to be affected by the detector and background non-uniformity. Depending on the dithering pattern, these effects may be reduced or amplified, leading to different spectral shapes obtained with different methods. The influence of dithering strategy on the spectral results will be studied in future in connection with the non-uniformity investigations. Also the count rate discrepancies appearing for methods based on images need further studies.

Results obtained for Crab are confirmed by the tests performed for weaker objects. For on-axis observation all methods give the same spectra even for sources as weak as 10 mCrab. Analysis of data collected with large offset angles , e.g. GPS, should be performed with a special care. If it is possible, the data set should be limited to offset angles smaller than 10 degrees (FCFOV) and the influence of detector/background non-uniformity on the results should be reduced via averaging of spectra obtained for different pointings.

In summary, there is no need to use methods other than the standard spectral extraction method for not too large (< 10 degrees) offset angles. Alternative methods do not lead to a better spectral shape in this case and produce systematically lower fluxes. However, this differences are not larger than the current uncertainty of ISGRI absolute calibration. For sources observed at larger offset angles method based on averaging fluxes obtained for given pixel in individual science window sky images is recommended. In this case the standard spectral extraction usually produces false, too hard spectra, for objects not bright enough to be well separated from the background.

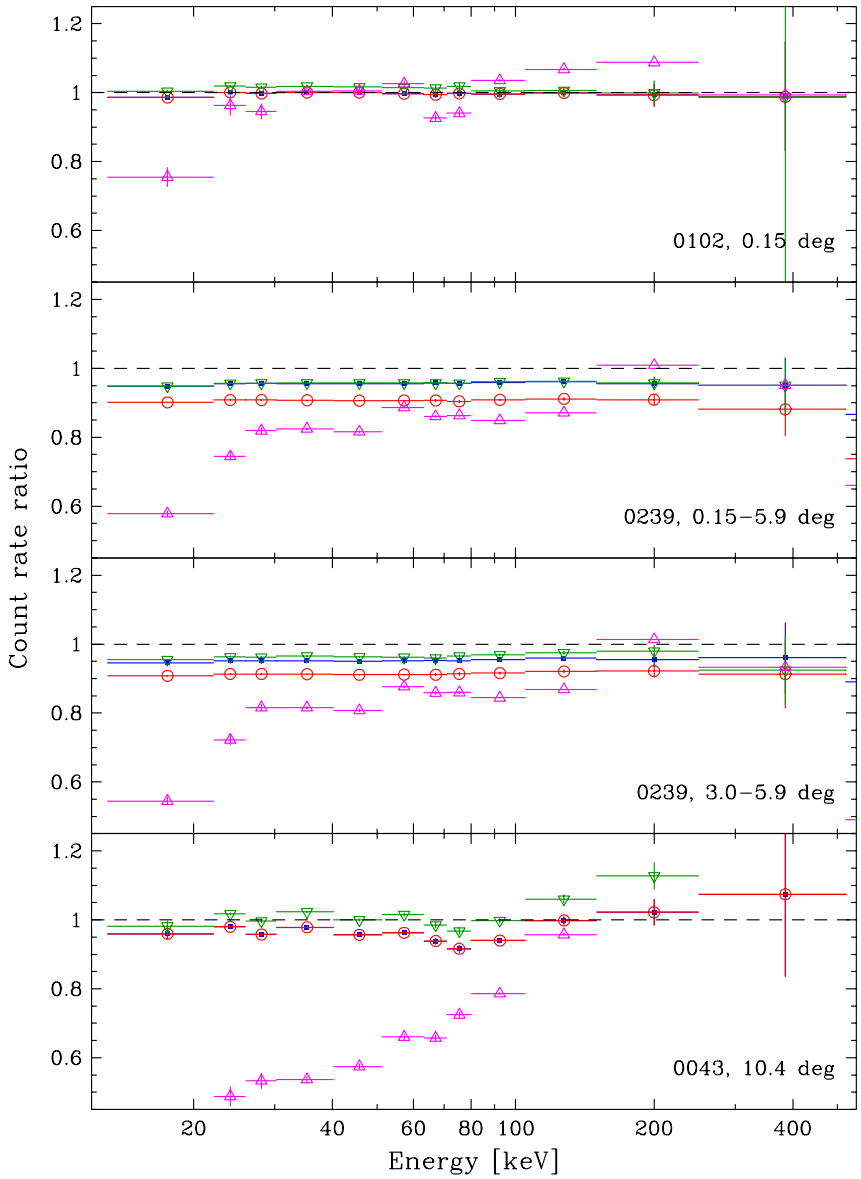

Fig. 1.— Count rate ratios obtained for tested method and the standard one, results for observations of Crab in revolutions 0043, 0102 and 0239. Blue dots - method IA, red circles - MI, green triangles - MR, magenta triangles - S2.

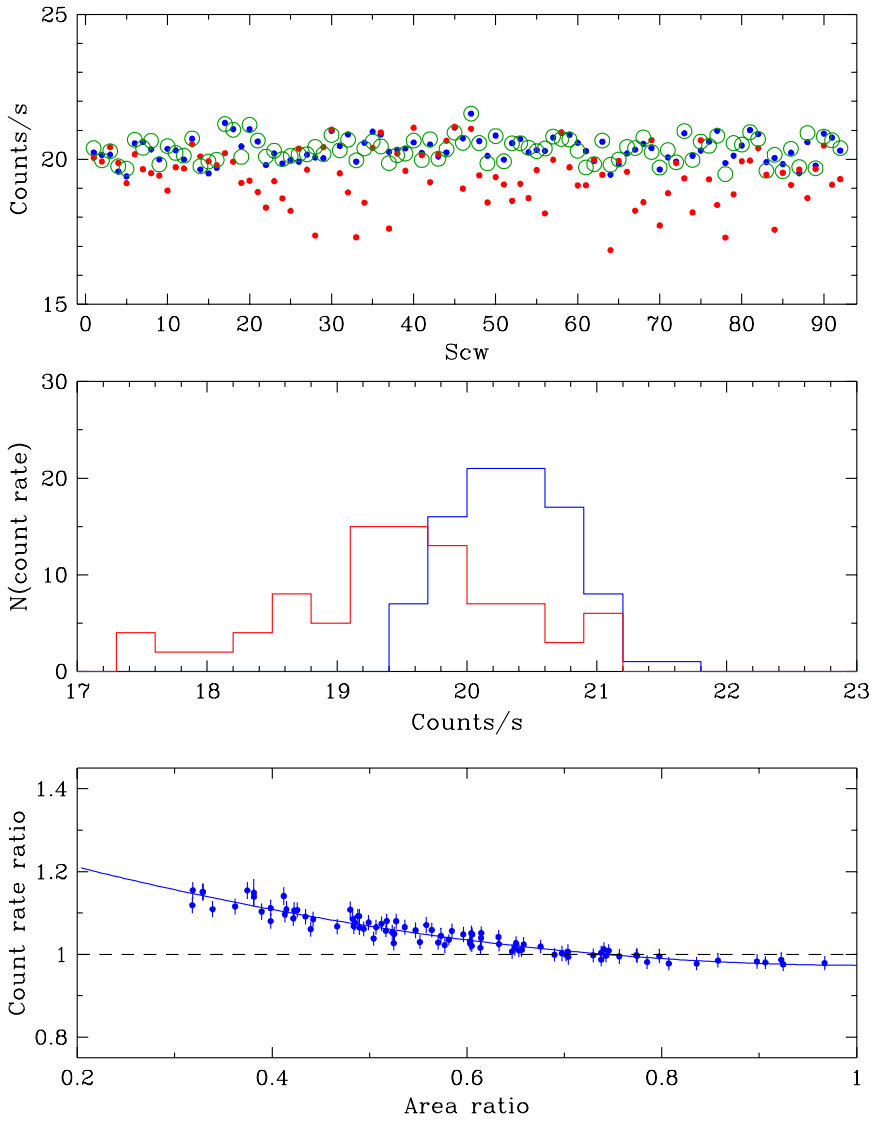

Fig. 2.— Upper panel: Count rates obtained for all ScWs from Crab observation in Rev. 0239, offset angle 0.15-5.9 degrees. Blue dots - standard method S1, red dots - method IA (fluxes from images), green circles - fluxes extracted from PSF fitting applied to images. Middle panel: Distributions of count rates obtained for S1 (blue) and IA (red) methods. Lower panel: The ratio between S1 and IA count rates plotted against pixel area ratios (see the text for explanation). Blue line shows the second order polynomiale fitted to these data.

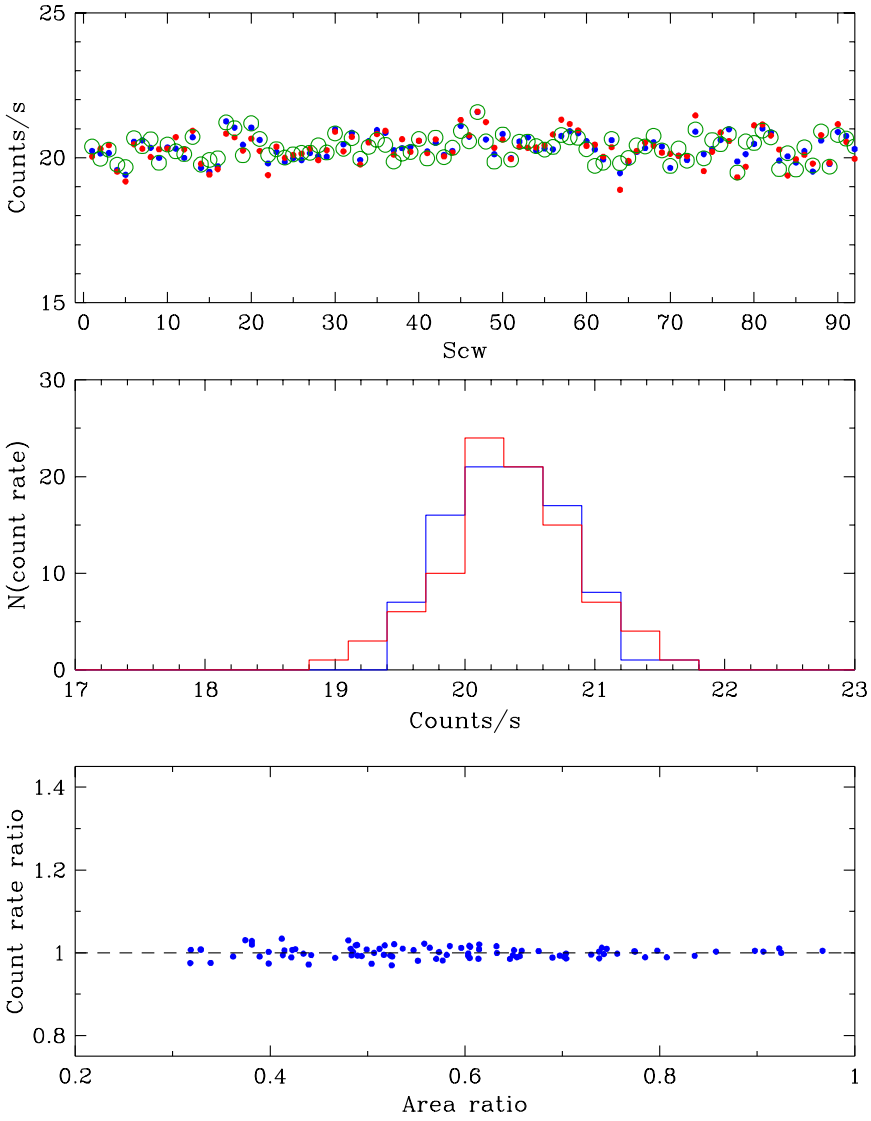

Fig. 3.— The same as in Figure 2 but with the results of method IA corrected.

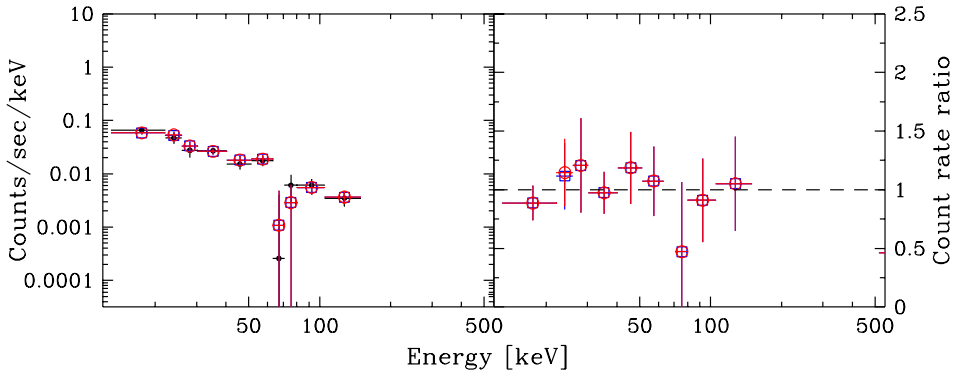

Fig. 4.— Spectra and count rate ratios obtained for Mrk 509 observation from revolution 0070. Black dots - standard method S1, blue squares - IA, red circles - MI.

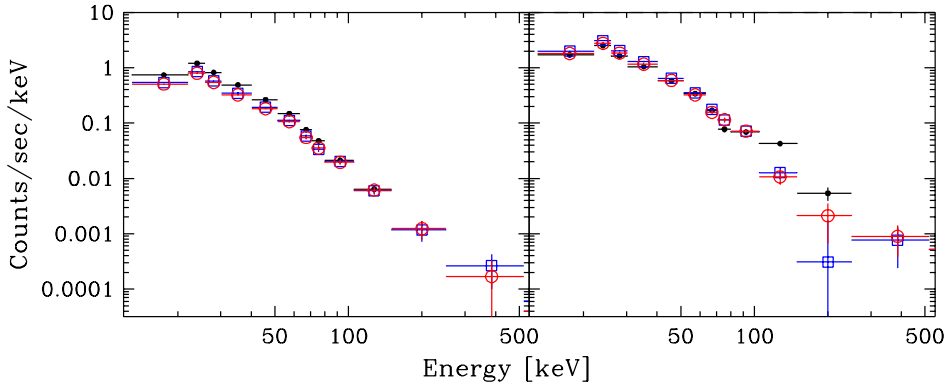

Fig. 5.— Spectra of 4U 1700-377 from revolution 0100 (left) and 0116,0118 (right). Results for different methods are shown with the same colors as in Mrk 509 case.

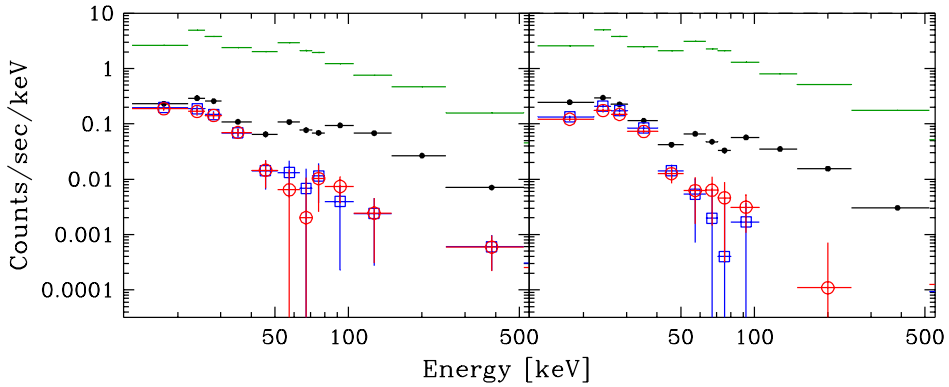

Fig. 6.— Spectra of H 1538-522 from revolution 0100 (left) and 0116,0118 (right). Results for different methods are shown with the same colors as in Mrk 509, whereas background extracted with standard method is presented with green.